

Oxide Ionic Conductivity of Apatite Type $\text{Nd}_{9.33}(\text{SiO}_4)_6\text{O}_2$ Single Crystal

Susumu Nakayama,^{a*} Masatomi Sakamoto,^b Mikio Higuchi,^c Kohei Kodaira,^c Mineo Sato,^d Shinichi Kakita,^e Toshihisa Suzuki^e and Katsuhiko Itoh^e

^aDepartment of Applied Chemistry and Biotechnology, Niihama National College of Technology, Niihama, 792-8580, Japan

^bDepartment of Material and Biological Chemistry, Faculty of Science, Yamagata University, Yamagata 990-8560, Japan

^cDepartment of Materials Technology, Graduate School of Engineering, Hokkaido University, Sapporo, 060-8628, Japan

^dDepartment of Chemistry and Chemical Engineering, Faculty of Engineering, Niigata University, Niigata, 950-2181, Japan

^eDaiichi Kigenso Kagaku Kogyo Co., Ltd., Osaka 541-0043, Japan

(Received 2 June 1998; accepted 1 September 1998)

Abstract

Single crystal of hexagonal apatite type $\text{Nd}_{9.33}(\text{SiO}_4)_6\text{O}_2$ which is an oxide ionic conductor was prepared by the FZ method and an anisotropy of its conductivity was investigated. The conductivity of a parallel component to a c-axis ($2.1 \times 10^{-8} \text{ S cm}^{-1}$ at 30°C) was higher about one order of magnitude, compared with that of perpendicular component. © 1999 Elsevier Science Limited. All rights reserved

Keywords: apatite, ionic conductivity, electrical properties, silicate, anisotropy.

1 Introduction

A number of oxide ionic conductors having potential applications to sensors, fuel cells and oxygen pumps have been prepared. Among these ionic conductors, it is well known that the fluorite type oxides such as $(\text{ZrO}_2)_{0.9}(\text{Y}_2\text{O}_3)_{0.1}$ ($6.3 \times 10^{-4} \text{ S cm}^{-1}$ at 500°C), $(\text{CeO}_2)_{0.79}(\text{Er}_2\text{O}_3)_{0.21}$ ($1.3 \times 10^{-3} \text{ S cm}^{-1}$ at 500°C) and $(\text{Bi}_2\text{O}_3)_{0.8}(\text{Er}_2\text{O}_3)_{0.2}$ ($2.2 \times 10^0 \text{ S cm}^{-1}$ at 500°C) and the perovskite type oxides such as $\text{La}_{0.9}\text{Sr}_{0.1}\text{Ga}_{0.8}\text{Mg}_{0.2}\text{O}_3$ ($6.3 \times 10^{-3} \text{ S cm}^{-1}$ at 500°C) and $\text{BaCe}_{0.8}\text{Gd}_{0.2}\text{O}_3$ ($2.0 \times 10^{-4} \text{ S cm}^{-1}$ at 200°C and $1 \times 10^{-2} \text{ S cm}^{-1}$ at 500°C) show the high conductivities.^{1–5} Besides these conductors, we, very recently, prepared the new type oxide ionic conductors, $\text{RE}_X\text{Si}_6\text{O}_{12+1.5X}$ (RE = La, Pr, Nd, Sm, Gd or Dy; $X=8–11$) and found their high conductivities at low temperature.⁶ The conductivities

of $\text{La}_{10}\text{Si}_6\text{O}_{27}$ at 200, 300 and 500°C were 1.3×10^{-5} , 2.4×10^{-4} and $4.3 \times 10^{-3} \text{ S cm}^{-1}$, respectively, and the activation energy was estimated at 62 kJ mol^{-1} . The major phase in $\text{RE}_X\text{Si}_6\text{O}_{12+1.5X}$ has a hexagonal apatite structure (space group: $\text{P6}_3/\text{m}$) with a composition of $\text{RE}_X(\text{SiO}_4)_6\text{O}_{1.5X-12}$ in the range of $X=8–9.33$.⁷ In this apatite structure, the oxygen ions, which are not a member of the SiO_4 tetrahedron, are located at the 2a site of the channel along the c-axis, and thence are responsible for the ionic conduction, as can be seen in Fig. 1.^{6,7} Thus, an anisotropy of the conduction is expected between parallel and perpendicular components to the c-axis. An investigation of such anisotropy by the use of single crystal will give basic and useful informations about the development of new functional materials.

In the present work, we will report the preparation of single crystal of $\text{Nd}_{9.33}(\text{SiO}_4)_6\text{O}_2$ by the floating zone (FZ) method and its anisotropy of ionic conduction.

2 Experimental

Single crystal was prepared as follows: Nd_2O_3 (99.9%) and SiO_2 (99.9%) as the starting materials were mixed in ethanol with a ball-mill and plastic pot. The mixture was dried and then calcined in air at 1500°C for 2 h. After the resultant powder was again ball-milled into fine powders and dried, a rod was prepared under 100 MPa with the cold isostatic press and sintered in air at 1650°C for 2 h. The single crystal growth was accomplished at 1900°C in the N_2 stream by the FZ method using an infrared furnace, where the growth and rotation rates were

*To whom correspondence should be addressed. Fax: +81-897-37-1245; e-mail: nakayama@chem.niihama-nct.ac.jp

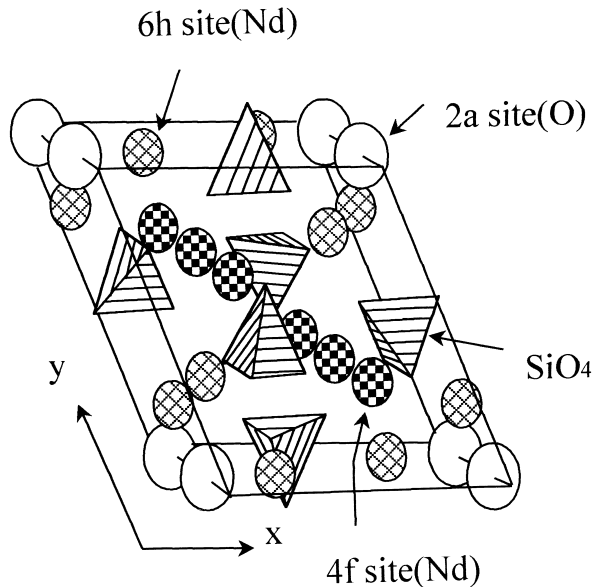


Fig. 1. Hexagonal apatite structure proposed for $\text{Nd}_{9.33}(\text{SiO}_4)_6\text{O}_2$ single crystal.⁶

5 mm h^{-1} and 80 rpm , respectively. Two kinds of sample discs for electrical measurements (the conductivity components parallel and perpendicular to the c -axis of single crystal of $\text{Nd}_{9.33}(\text{SiO}_4)_6\text{O}_2$ and were manufactured from this single crystal rod, after the crystal-axes were determined by X-ray diffraction method. The diameter and thickness of disc were 5 and 1 mm , respectively. After both sides of disc were coated with Pt paste, the disc was baked at 950°C . The electrical properties were measured using YHP 4276A and 4277A LCZ meters. The electromotive force, EMF, of the O_2 concentration cell, $\text{O}_2 + \text{N}_2$, Pt/ $\text{Nd}_{9.33}(\text{SiO}_4)_6\text{O}_2$ single crystal/Pt, air, was measured using an Advantest TR8652 electrometer in the partial pressure range of 1×10^3 to $8 \times 10^4 \text{ Pa}$ by the method reported in the previous paper,⁶ where the single crystal used is the disc manufactured for the measurement of conductivity component parallel to the c -axis.

3 Results and Discussion

Figure 2 shows the appearance of a as-grown single crystal of $\text{Nd}_{9.33}(\text{SiO}_4)_6\text{O}_2$. The color is dark purple characteristic of neodymium(III) ion. It was confirmed from X-ray diffraction measurement



Fig. 2. Appearance of as-grown $\text{Nd}_{9.33}(\text{SiO}_4)_6\text{O}_2$ single crystal.

that the single crystal is a single phase of apatite structure with space group $\text{P6}_3/\text{m}$.

Conductivities were determined by a complex plane impedance analysis. Typical complex impedance plots for the components parallel and perpendicular to the c -axis of single crystal of $\text{Nd}_{9.33}(\text{SiO}_4)_6\text{O}_2$ and for $\text{Nd}_{10}\text{Si}_6\text{O}_{27}$ ceramic are shown in Fig. 3. Hereafter, σ_{\parallel} and σ_{\perp} are defined as the conductivity components parallel and perpendicular to the c -axis, respectively. In the lower temperatures, the low-frequency plots are represented by a spur and the high frequency plots by a semicircle which passes through the origin. When temperature was increased, the semicircle probably corresponding to the electrolyte itself diminished and only a spur probably arising from electrolyte-electrode behavior was observed. From these results, the conductivity was determined by the extrapolation to zero reactance of the complex impedance plot. The conductivity data were parameterized by the Arrhenius equation,

$$\sigma T = \sigma_0 \exp(-E/kT)$$

where σ , σ_0 , E , k and T are the conductivity, pre-exponential factor, activation energy, Boltzmann constant and absolute temperature, respectively. Arrhenius plots of the σ_{\parallel} and σ_{\perp} of single crystal of $\text{Nd}_{9.33}(\text{SiO}_4)_6\text{O}_2$ are shown in Fig. 4, together with plots of $\text{Nd}_{10}\text{Si}_6\text{O}_{27}$ ceramic sintered at 1750°C .⁶ Table 1 summarizes the estimated electrical parameters. The σ_{\parallel} -value is higher about ten times than the σ_{\perp} -value. The activation energy of σ_{\parallel} (defined as E_{\parallel} hereafter) in the higher temperature is lower than that of σ_{\perp} (defined E_{\perp} hereafter), though the E_{\parallel} -value in the lower

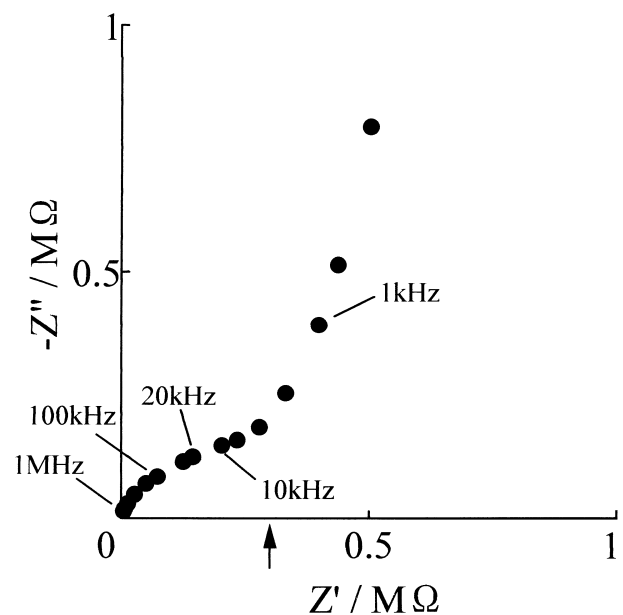


Fig. 3. Complex impedance plot of $\text{Nd}_{9.33}(\text{SiO}_4)_6\text{O}_2$ single crystal (component parallel to c -axis) at 100°C .

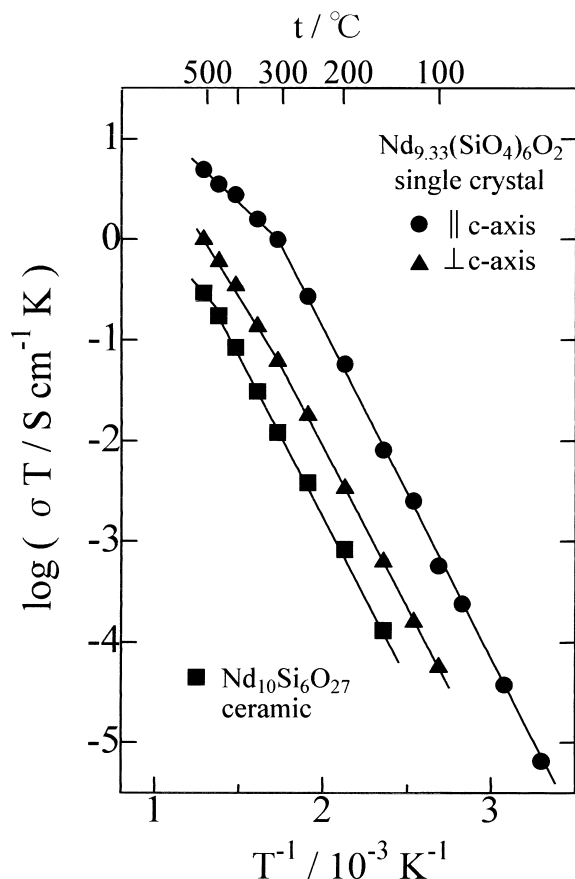


Fig. 4. Temperature dependence of conductivity.

Table 1. Parameters of electrical properties

	Activation energy/ kJ mol^{-1}	Conductivity/ S cm^{-1}		
		100°C	300°C	500°C
$\text{Nd}_{9.33}(\text{SiO}_4)_6\text{O}_2$ single crystal				
c-axis	60 (30)	1.5×10^{-6}	1.7×10^{-3}	6.4×10^{-2}
⊥ c-axis	59 (48)	1.5×10^{-7}	1.1×10^{-4}	1.3×10^{-3}
$\text{Nd}_{10}\text{Si}_6\text{O}_{27}$ ceramic	59 (47)	—	2.1×10^{-5}	3.8×10^{-4}

Parentheses denote the activation energy estimated in a higher temperature region.

temperature is equal to the E_{\perp} -value. Thus, as was expected, an anisotropy of conductivity was confirmed for the single crystal of $\text{Nd}_{9.33}(\text{SiO}_4)_6\text{O}_2$. It is surprising that the present σ_{\parallel} -value at 30°C is $2.1 \times 10^{-8} \text{ S cm}^{-1}$ which is higher compared with the $(\text{ZrO}_2)_{0.9}(\text{Y}_2\text{O}_3)_{0.1}$, $(\text{CeO}_2)_{0.79}(\text{Er}_2\text{O}_3)_{0.21}$, $(\text{Bi}_2\text{O}_3)_{0.8}(\text{Er}_2\text{O}_3)_{0.2}$, $\text{La}_{0.9}\text{Sr}_{0.1}\text{Ga}_{0.8}\text{Mg}_{0.2}\text{O}_3$ and $\text{BaCe}_{0.8}\text{Gd}_{0.2}\text{O}_3$ ceramics which are known to exhibit relatively high oxide ionic conductivities. Furthermore, the σ_{\parallel} -value of the present $\text{Nd}_{9.33}(\text{SiO}_4)_6\text{O}_2$ is higher, about 80–170 times than that of conductivity of $\text{Nd}_{10}\text{Si}_6\text{O}_{27}$ ceramic. The appearance of inflection point in the Arrhenius plot may be due to the change in structures of oxygen vacancies which are ordered at lower temperature and disordered at the higher temperature.

Table 2. Theoretical and experimental Nernstian slopes and electron transfer number (n) for O_2 gas concentration cell using $\text{Nd}_{9.33}(\text{SiO}_4)_6\text{O}_2$ single crystal (disc manufactured for measurement of conductivity component parallel to c-axis) as a solid electrolyte

Temperature/ $^\circ\text{C}$	Slope/ mV decade^{-1}		
	Theoretical ($n=4$)	Observed	n
250	25.91	18.5	5.9
300	28.39	22.4	5.1
350	30.87	30.9	3.9
400	33.35	34.5	3.9
500	38.30	37.2	4.1

Since the σ_{\parallel} -value is very high as described above, the property as an O_2 gas concentration cell was investigated using the cell mentioned in the experimental section. The EMF between two electrodes obeys the Nernst equation,

$$\text{EMF} = (RT/nF) \ln(P_{\text{O}_2}/P_{\text{O}_2}')$$

where R , T , n , F , P_{O_2} and P_{O_2}' are the gas constant, absolute temperature, electron transfer number, Faraday constant, partial pressure of O_2 at the measuring electrode, and partial pressure of O_2 ($P_{\text{O}_2}' = 2.1 \times 10^4 \text{ Pa}$) at the reference electrode, respectively. Table 2 summarizes the theoretical and experimental Nernstian slopes and the electron transfer numbers at each temperature. The observed EMF values are in good agreement with the theoretical values calculated assuming that n is 4, indicating that the response must be derived from the four electron reaction associated with O_2 molecules at the electrodes above 350°C . Furthermore, the conductivity determined by the dc method was considerably lower than that determined by the ac method. (The lower dc conductivity is probably attributable to the formation of the electric double-layer of electrolyte–electrode boundary.) The conductivity in a moist atmosphere was the same as that in a dry atmosphere. These results suggest that electrons, holes and protons are not the major charge carrier in the single crystal of $\text{Nd}_{9.33}(\text{SiO}_4)_6\text{O}_2$, though it can not be clarified at present that oxide ions are the conductive ions.

Further studies of the relationship between the electrical properties and the oxide ion vacancy or the oxide ion concentration are in progress, in order to understand the mechanism of oxide ionic conduction in more detail.

Acknowledgements

The authors thank Mr R. Yajima, a former managing director of Shinagawa Refractories Co., Ltd., for his helpful advice.

References

1. Brune, A., Lajavardi, M., Fislser, D. and Wagner Jr, J. B., The electrical conductivity of yttria-stabilized zirconia prepared by precipitation from inorganic aqueous solutions. *Solid State Ionics*, 1998, **106**, 89–101.
2. Hong, S. J., Mehta, K. and Virkar, A. V., Effect of microstructure and composition on ionic conductivity of rare-earth oxide-doped ceria. *J. Electrochem. Soc.*, 1998, **145**, 638–647.
3. Azad, A. M., Larose, S. and Akbar, S. A., Review—Bismuth oxide-based electrolytes for fuel cells. *J. Mater. Sci.*, 1994, **29**, 4135–4151.
4. Ishihara, T., Matsuda, H. and Takita, Y., Doped LaGaO₃ perovskite type oxide as a new oxide ionic conductor. *J. Am. Chem. Soc.*, 1994, **116**, 3801–3803.
5. Taniguchi, N., Yasumoto, E., Nakagiri, Y. and Gamo, T., Sensing properties of an oxygen sensor using BaCe_{0.8}Gd_{0.2}O₃ ceramics as electrolytes. *J. Electrochem. Soc.*, 1998, **145**, 1744–1748.
6. Nakayama, S. and Sakamoto, M., Electrical properties of new type high oxide ionic conductor RE₁₀Si₆O₂₇ (RE = La, Pr, Nd, Sm, Gd, Dy). *J. Eur. Ceram. Soc.*, 1998, **18**, 1413–1418.
7. Felsche, J., Rare earth silicates with the apatite structure. *J. Solid State Chem.*, 1972, **5**, 266–275.